

Table S1 Tropical and extratropical volcanic eruption event years used for SEA in Figure 6. List of the largest volcanic eruptions during the period 1461–1900 are based sulfate records from a collection of ice core records from Greenland and Antarctica. Event years, names, and locations derive from the Volcanoes of the World database (v. 5.1.7; 26 Apr 2024) provided by the Global Volcanism Program and are listed in (93, 87, 88). We also include instrumental-period eruptions since 1900 CE. Temperature anomalies are included for each event either during the eruption year (extratropical) or year following the eruption (tropical).

Volcano	Eruption Year	Temp °C	Location
Bároarbunga (Veidivötn)	1477	-0.29	Extratropical
Hekla	1510	-0.97	Extratropical
Colima	1585	-0.42	Tropical
Nevado del Ruiz	1595	-1.01	Tropical
Huaynапutina	1600	-0.92	Tropical
Parker	1641	-1.3	Tropical
Shikotsu (Tarumai)	1667	-1.51	Extratropical
Gamkonora	1673	-1.05	Tropical
Fujisan	1707	-0.20	Extratropical
Katla	1721	-0.15	Extratropical
Shikotsu (Tarumai)	1739	0.55	Extratropical
Katla	1755	-1.11	Extratropical
Hekla (Bjallagigar)	1766	-1.84	Extratropical
Grímsvötn (Laki)	1783	-0.70	Extratropical
Tambora	1815	-0.80	Tropical
Galunggung	1822	-0.28	Tropical
Babuyan Claro	1831	-0.48	Tropical
Cosiguina	1835	-1.81	Tropical
Toya (O-Usu)	1853	0.37	Extratropical
Hokkaido-Komagatake	1856	-0.80	Extratropical
Makian	1861	-0.20	Tropical
Grímsvötn	1873	-0.67	Extratropical
Askja (ÖskjuvatnCaldera)	1875	-0.13	Extratropical
Krakatau	1883	-0.88	Tropical
Okataina (Tarawera)	1886	-1.05	Extratropical
Novarupta	1912	-1.16	Extratropical
Agung	1963	-0.65	Tropical
El Chichon	1982	0.69	Tropical
Pinatubo	1991	-0.83	Tropical

Table S2 Chronology site information used in the MANE T_{Mar-Sep} reconstruction. Site statistics and location correspond with Figure 1. All collections are *T. canadensis* except for Cape Natural Research Area (*P. rubens*). r_{target} = correlation coefficient versus target instrumental data (hatched area from Figure 1), r_{local} = correlation coefficient versus local data, β = beta weight, rbar = average Pearson's correlation between all measured series in the chronology, DOI=hyperlink to International Tree Ring Data Bank. r_{local} calculated with T_{Mar-Sep} data from the nearest CRU TS 4.07 0.5°grid point to each site Lat/Long location.

Site Name	r_{target}	β	r_{local}	Lat (N°)	Long. (W°)	Start	End	rbar	DOI
Alan Seeger Natural Area	0.59	0.09	0.54	40.70	-77.75	1609	2013	0.33	—
Alander Mountain	0.68	0.12	0.69	42.09	-73.51	1779	2005	0.42	—
Bear Run Nature Preserve	0.65	0.11	0.50	39.90	-79.44	1646	2020	0.34	—
Bigelow Pond	0.46	0.06	0.36	41.96	-73.22	1655	1986	0.33	CT001
Bigelow Pond Recollect	0.44	0.05	0.38	41.96	-73.22	1646	2012	0.36	CT004
Boody Pond	0.44	0.05	0.42	44.57	-69.98	1747	2012	0.28	ME042
Boody Pond Update	0.56	0.09	0.53	44.57	-69.98	1768	2022	0.45	—
Bradbury Mountain State Park	0.41	0.05	0.46	43.90	-70.18	1896	2012	0.46	ME043
Cape Research Natural Area	0.52	0.06	0.50	43.81	-72.98	1811	2009	0.35	—
Dingmans Falls	0.44	0.05	0.49	41.23	-74.89	1607	2020	0.28	—
East Branch Swamp Natural Area	0.37	0.04	0.46	41.23	-77.77	1511	1981	0.30	PA004
Ferncliff Peninsula Natural Area	0.43	0.05	0.51	39.87	-79.50	1623	2020	0.35	—
Gibbs Brook	0.63	0.11	0.70	44.22	-71.40	1660	2013	0.34	NH002
Granville Gulf State Forest	0.38	0.04	0.39	44.02	-72.83	1633	1981	0.35	VT002
Granville Gulf State Forest Update	0.57	0.09	0.61	44.02	-72.83	1785	2020	0.45	—
Little Concord Pond	0.45	0.07	0.48	44.43	-70.53	1681	2012	0.36	ME045
Little Concord Pond Update	0.47	0.07	0.42	44.43	-70.53	1761	2022	0.50	—
Mattawamkeag Wilderness Park	0.45	0.05	0.46	45.52	-68.28	1677	2012	0.46	ME046
Nancy Brook	0.48	0.07	0.52	44.12	-71.37	1627	2021	0.31	—
Pack Forest	0.57	0.09	0.64	43.56	-73.81	1542	2021	0.29	—
Paradise Point Trail	0.42	0.05	0.40	43.70	-71.78	1643	2021	0.39	—
Ricketts Glen State Park	0.63	0.10	0.65	41.31	-76.28	1621	2020	0.36	—
Salt Springs State Park	0.28	0.02	0.31	41.91	-75.87	1620	1981	0.40	PA011
Snyder Middleswarth Natural Area	0.51	0.08	0.55	40.81	-77.29	1762	2020	0.32	—
Spruce Glen	0.64	0.11	0.68	41.73	-74.24	1654	2021	0.29	—
Swallow Falls State Park	0.49	0.06	0.47	39.50	-79.42	1694	2020	0.30	—
Sweetroot Natural Area	0.45	0.05	0.46	39.84	-78.52	1612	1981	0.27	PA012
Tionesta	0.49	0.05	0.51	41.50	-79.43	1461	1978	0.28	PA013
Tionesta Update	0.62	0.11	0.63	41.50	-79.43	1603	2021	0.26	—

Table S3 Nested reconstruction model statistics. Northeast US $T_{\text{Mar-Sep}}$ nested reconstruction model statistics, including the common period model (CP) with backward (B) and forward (F) model nests for the period 1461–2021 CE. # CRNS=number of tree-ring chronologies, # CORES=number of individual tree cores, CR^2/VR^2 =calibration/verification period coefficient of determination, VRE/VCE=verification period reduction of error/coefficient of efficiency, RMSE=root mean-squared error

Nest	Period	# CRNS	# CORES	CR^2	VR^2	VRE	VCE	RMSE
F8	2020-2021	2	55	0.18	0.10	0.11	0.06	0.68
F7	2014-2020	8	227	0.46	0.38	0.41	0.38	0.55
F6	2012-2013	15	406	0.50	0.45	0.46	0.38	0.52
F5	2006-2012	16	426	0.56	0.45	0.47	0.44	0.51
F4	1987-2005	17	466	0.57	0.52	0.54	0.52	0.48
F3	1982-1986	23	597	0.53	0.52	0.53	0.51	0.46
F2	1979-1981	24	812	0.61	0.65	0.65	0.64	0.41
F1	1977-1978	28	947	0.62	0.66	0.67	0.66	0.41
CP	1896-1976	29	983	0.62	0.67	0.67	0.66	0.41
B1	1790-1895	28	801	0.62	0.67	0.67	0.66	0.41
B2	1780-1789	27	415	0.62	0.68	0.67	0.66	0.41
B3	1770-1779	26	395	0.61	0.67	0.67	0.66	0.42
B4	1750-1769	23	360	0.62	0.70	0.69	0.68	0.41
B5	1700-1749	22	300	0.62	0.69	0.69	0.68	0.41
B6	1690-1699	21	168	0.62	0.68	0.68	0.67	0.41
B7	1680-1689	19	144	0.63	0.68	0.68	0.67	0.41
B8	1660-1679	18	116	0.63	0.67	0.67	0.67	0.41
B9	1650-1659	15	77	0.59	0.63	0.63	0.62	0.43
B10	1640-1649	12	61	0.58	0.62	0.63	0.62	0.44
B11	1630-1639	11	52	0.53	0.63	0.63	0.62	0.43
B12	1620-1629	8	46	0.56	0.61	0.61	0.60	0.44
B13	1610-1619	6	39	0.55	0.63	0.63	0.62	0.45
B14	1550-1609	3	28	0.41	0.47	0.47	0.45	0.51
B15	1520-1549	2	9	0.20	0.37	0.32	0.30	0.60
B16	1461-1519	1	5	0.18	0.36	0.28	0.26	0.60

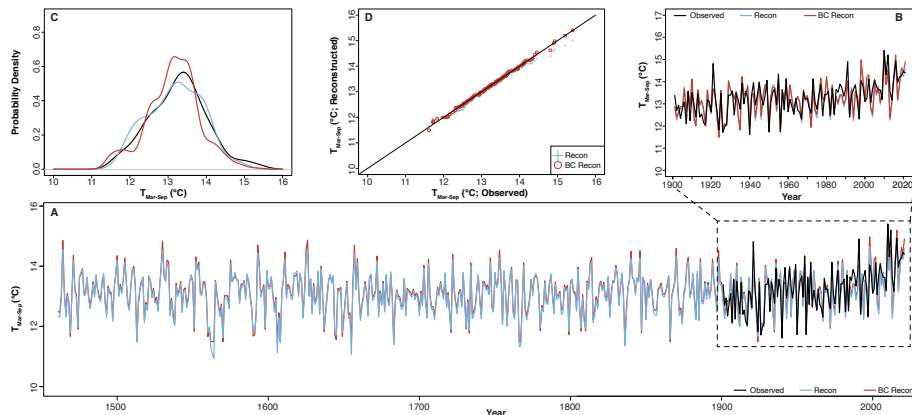


Fig. S1 MANE $T_{\text{Mar-Sep}}$ reconstruction bias correction. (A) Time series of uncorrected (blue) and bias-corrected (BC; red) $T_{\text{Mar-Sep}}$ reconstruction spanning 1461–2021 CE plotted with instrumental Mar-Sep CRU TS4.07 $T_{\text{Mar-Sep}}$ data during the period 1901–2021 (black) [zoom inset shown as (B)]. (C) Probability density functions for the uncorrected (blue) and bias-corrected and instrumental data (black). (D) Quantile-quantile plot of the uncorrected (blue) and bias-corrected (red) reconstructions.

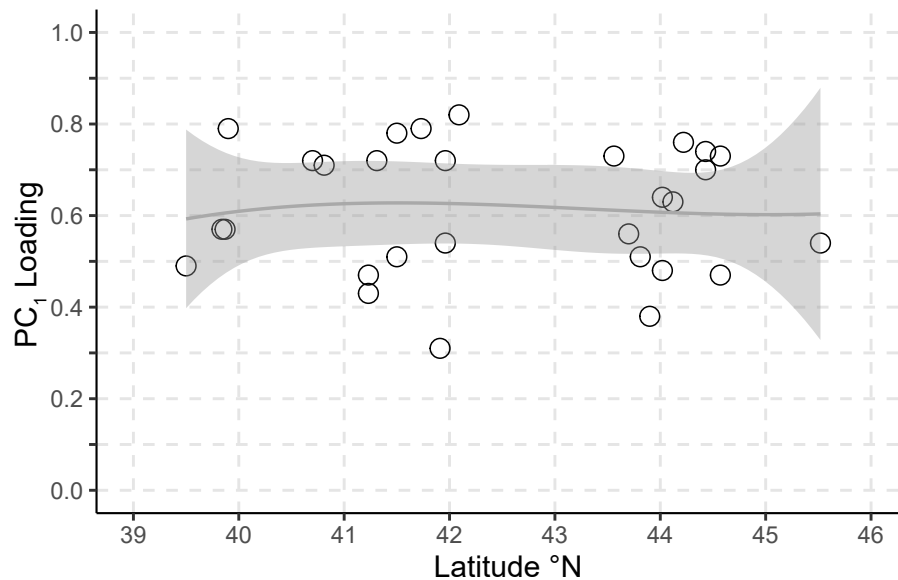


Fig. S2 MANE LWBI network PC₁ loadings versus latitude. PC₁ loadings of the 29 predictor sites plotted against site latitude. Solid gray line is a 2nd-order polynomial function with 2- σ error (gray envelop) to show non-linear relationship between latitude and loadings.

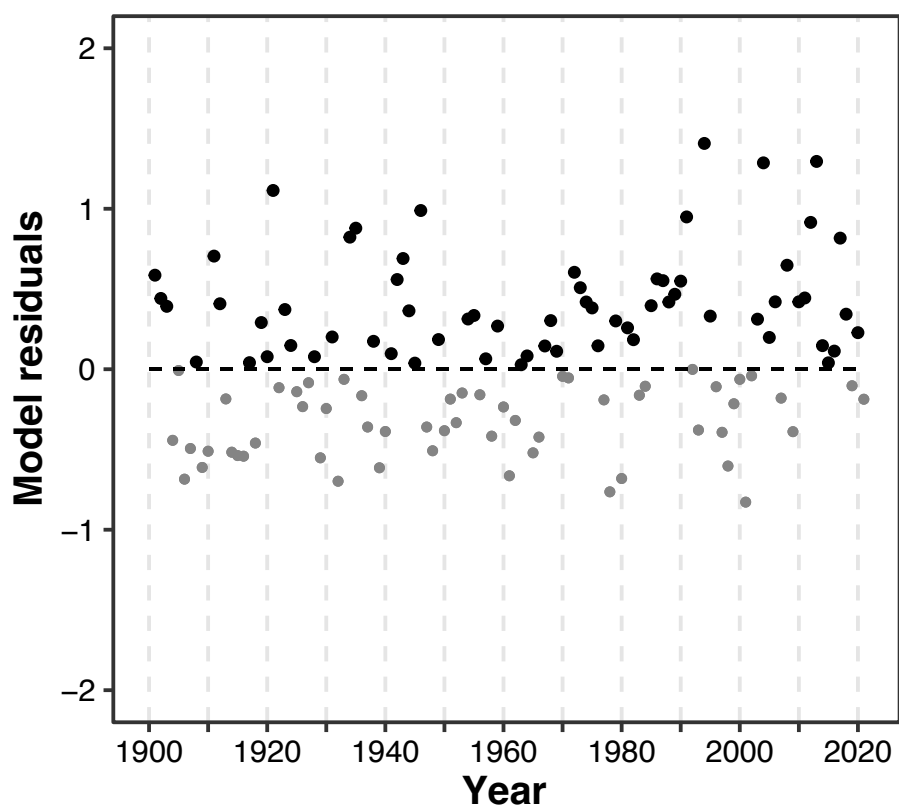


Fig. S3 MANE T_{Mar-Sep} reconstruction model (bias corrected) residuals. Predicted values subtracted from actual values (CRU TS4.07; (43)) during the period 1901-2021. Positive (black dot) values are underpredictions and negative (gray dot) values are overpredictions.

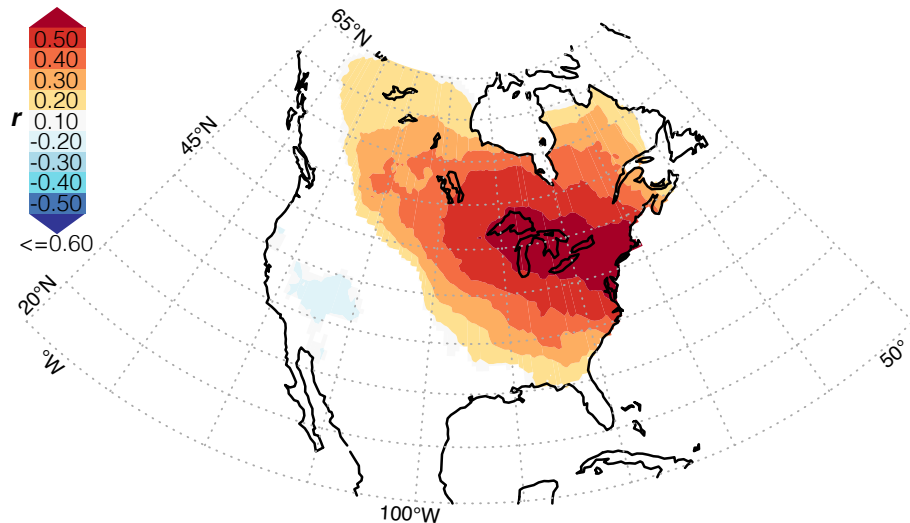


Fig. S4 Spatial footprint of the MANE T_{Mar-Sep} reconstruction. Map showing the spatial Pearson's correlation ($p<0.01$; 1st-differenced) between PC₁ of the LWBI records included in the MANE network and gridded CRU TS4.07 T_{Mar-Sep} during the period 1901–1976. Site information for each location is available in Table S2.